

# CORRELATION ANALYSIS OF SEISMIC WAVES ON RECORD SECTIONS FOR EARTHQUAKES IN THE JAPAN REGION

著者	KAKUTA Toshiki
journal or publication title	鹿児島大学理学部紀要. 地学・生物学
volume	22
page range	89-117
別言語のタイトル	日本周辺域に発生した地震気象の相関解析
URL	<a href="http://hdl.handle.net/10232/00006946">http://hdl.handle.net/10232/00006946</a>

## CORRELATION ANALYSIS OF SEISMIC WAVES ON RECORD SECTIONS FOR EARTHQUAKES IN THE JAPAN REGION

Toshiki KAKUTA

(Received August 30, 1989)

### Abstract

Correlation analyses of seismic waves were made on several record sections for accurate measurements of slowness along arc systems in the Japan region. Slownesses derived from shallow depth earthquakes were 13.3-13.7 s/deg for events occurring in the northeast and 13.9-14.0 s/deg for an event in the southwest. They were almost consistent with  $P_n$  velocities from explosion seismic observations in the respective regions. Lag times versus distance corresponding to  $P_n$  branch extended continuously from  $4^\circ$  to  $18^\circ$  for very shallow earthquakes in the northeast region. Such a time curve was inconsistent with a model including a low velocity layer at a shallow depth.

A large later arrival of slowness 11.5-12.0 s/deg was observed at distances greater than  $10^\circ$  for the events in the northeast region : for very shallow and shallow depth earthquakes as well as for an intermediate depth earthquake. Considering its slowness and time lag curves for  $P_n$  branch extending to  $17-18^\circ$ , it was probably a phase reflected from a zone of velocity rapidly increasing near 400km depth. A similar arrival of low slowness was clearly noticed for the shallow earthquake in southwest Japan too. Since the time lag curve bent sharply from  $P_n$  branch to the low slowness branch of 11.7-11.9 s/deg at a distance near  $11^\circ$ , it was interpreted as a phase reflected at the upper boundary of the dipping lithosphere in the northeast Japan arc.

Weak phase  $P_r$  of 12.5 s/deg was detected by cross-correlations and cross-spectra for an intermediate depth event in the northeast region. Although its slowness was fit for a phase refracted from a zone immediately underlying the low velocity layer, it was not observed for shallow events. No clear time gap ascribable to the layer was not confirmed even on record sections of S waves.

### 1. Introduction

Examination of seismic waves on a record section is useful to estimate velocity structures reliably ; travel times and amplitudes are compared with theoretical ones as a function of epicentral distance for the first arrival as well as later arrivals. DRUMMOND *et al.* (1982) demonstrated evidence for a seismic discontinuity near 200 km depth under the continental margin of northwest Australia, analyzing record sections in a distance range from 1000 to 1700 km for three large earthquakes. This is a method generally pursued in the explosion seismology. There are, however, only a few examples applied to earthquakes

in a large scale.

Seismograms at a seismic array (JOHNSON, 1967 ; KANAMORI, 1967 ; FUKAO, 1977, for example) and a composite seismic record section at a limited network (JOHNSON, 1967 ; FROHLICH *et al.*, 1977) are often used to confirm theoretical models. Both methods are, however, intrinsically improper for lateral variations in a complicated structure : some other interpretation of seismic data may be possible in a short distance range ; it is difficult to estimate accurate shifts in origin times of earthquakes used in a composite record section.

In the present study, seismograms at stations spreading over the Japan region are examined in detail by a correlation analysis on a record section composed of many seismograms for a single earthquake. Such a section is more efficient in comparing waveforms and more suitable for directly verifying several phases than a composite record section.

## 2. Time Lags by the Methods of Cross-Correlation and Cross-Spectra

Cross-correlation is an effective method to check similarity in waveform and to detect a difference in phase lag between two wave trains. The normalized cross-correlation function between two discrete time series  $x_1(i)$  and  $x_2(i)$  at a sampling interval  $\Delta t$  is defined as follows :

$$C_{12}(j) = \sum_{i=-N}^N x_1(i)x_2(i+j) / [(2N+1)C_{11}(0)C_{22}(0)] \quad (1)$$

where  $C_{11}(0)$  and  $C_{22}(0)$  are auto-correlations. We obtain the time lag for the maximum of this function.

$$\tau = j\Delta t \quad (2)$$

On the other hand, time lags derived from cross-spectra are obtained as a function of frequency. Cross-spectra of wave trains  $x_1(i)$  and  $x_2(i)$  are given as

$$S_{12}(\omega) = E[(2\pi/T)X_1^*(\omega)X_2(\omega)] \quad (3)$$

$E[*]$  means the ensemble mean (HINO, 1977, p. 57) ;  $X_k(\omega)$  is the Fourier transform of a wave train  $x_k(i)$  and  $X_k^*(\omega)$  is its complex conjugate [ $x_k(i) = 0$ , if  $i < 0$  or  $i > T/\Delta t$ :  $k=1$  or  $2$ ]. Denoting the phase of  $X_1^*(\omega)$  by  $\theta_1(\omega)$  and that of  $X_2(\omega)$  by  $\theta_2(\omega)$ , we have the time lag :

$$\tau_{12}(\omega) = [\theta_1(\omega) - \theta_2(\omega)]/\omega + m(2\pi/\omega) \quad (4)$$

where  $m$  is an integer associated with the periodicity in time lags.

The integer  $m$  implies that the time lag for a spectral peak always include a periodic term. For a periodic wave train, maxima of cross-correlations appear at intervals of the period. We must then choose one out of the lags with reference to a slowness approximately inferred from a visual correlation on a record section. Both methods are consequently applicable when the period of the wave train is greater than the amount of scatter in the time lag data.

In the cross-correlation method, accuracy of the time lag depends on both of correlation function and phase difference. All the data were classified into four ranks according to a peak value of the function. Namely, *A*: 1.0-0.7, *B*: 0.7-0.5, *C*: 0.5-0.3, *D*: 0.3-0.0 (the data of *D* rank were omitted from the analysis). On the other hand, phase difference will be more accurately determined for a sharp peak than for a broad one. As a measure of error estimation, thus we used a peak-width, which is equivalent to a time difference between lags at a level reduced by 0.05 from the peak value.

Lengths of wave trains are determined to be roughly proportional to the period of the investigated phase. In the present study, setting a reference train for cross-correlation at a half to twice of the period, we correlated it with trains of half as long again as the reference. Cross-spectra were computed from a series of 200 to 400 in number; all the trains were equal in length to each other.

### 3. Correlation Analysis of P Waves on a Record Section

We analyzed seismograms of six earthquakes copied on film from those of smoked-paper recordings (only a few of ink system) at JMA stations (Fig. 1). Seismographs were mostly of the electromagnetic type (the undamped pendulum period  $T_0=5.0\pm 0.1$  s except for that of 10.0 s at NGS) but partly of the mechanical type of Wiechert ( $T_0=5.0\pm 0.3$  s) and Mainka ( $T_0=9.8\pm 0.4$  s at FKK for event 4 only). Optically enlarged seismograms up to about two minutes in length were sampled on a digitizer at variable intervals. We then modified the time series at intervals of 0.1 s, removing effects of the mechanical arm, zero

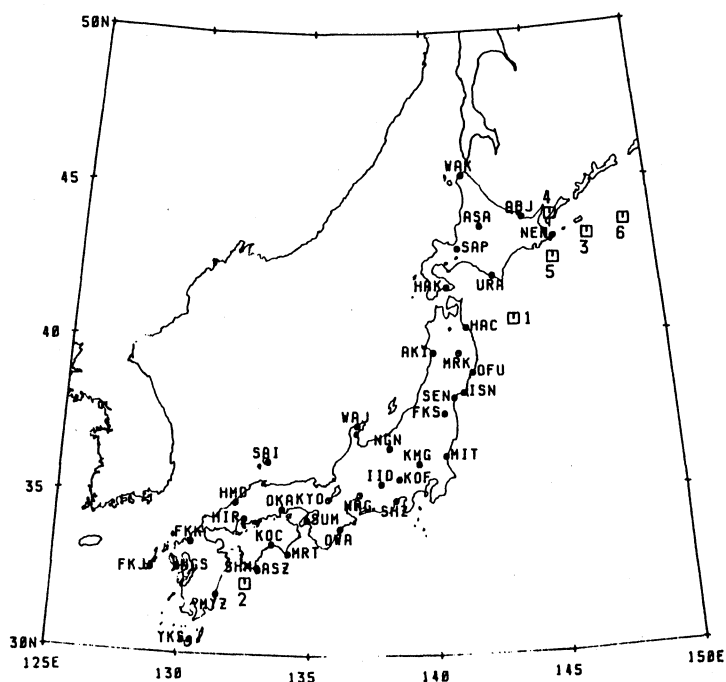


Fig. 1. Epicenters (square) and observation stations (circle) used in the present study. Integer assigned to the epicenter is the event number.

line shifts and linear trends. Filtration through a bandpass as well as reduction of instrumental effect was carried out in the frequency domain. The bandpass filter with cutoff frequencies of  $f_1$  and  $f_2$  was as follows :

$$\begin{aligned} H(f) &= \exp[-6.9(f_1/f-1)^2] && (f \leq f_1) \\ &= 1 && (f_1 < f < f_2) \\ &= \exp[-6.9(f/f_2-1)^2] && (f_2 \leq f) \end{aligned} \quad (5)$$

Vertical component seismograms were mainly analyzed for P waves. If a vertical component was lacked or obscured at a station, a radial component was substituted.

Begin by visually choosing a reference out of seismograms which exhibit well-marked characteristics of an investigated phase. By correlating any wave train including the phase with the reference, we obtain time lags for maxima of correlations or for spectral peaks. Time lags are plotted as a function of epicentral distance. Slowness for the phase is finally estimated by the method of least squares on the assumption that the lags versus distance are linear in a limited range.

For events 2 to 6 in Table 1, focal parameters were relocated on the basis of P arrivals within  $70^\circ$  in ISC and JMA bulletins. Some of the arrivals had been re-examined on JMA

Table 1. Focal parameters of events used to analyze seismic record sections.

No.	Origin time	Epicenter	Depth	M
1 May 16, 1968	0 h 48m 53.0 s	40.73°N 143.58°E	0km	7.9 JMA
2 Apr. 1, 1968	0 h 42m 03.9 s	32.38°N 132.46°E	36km	
	0 42 01.5	32.28 132.53	30	7.5 JMA
	0 42 04.2	32.48 132.28	37	6.2 ISC
3 May 31, 1964	0 h 40m 37.8 s	43.33°N 147.12°E	47km	
	0 40 35.7	43.27 147.23	60	6.7 JMA
	0 40 36.1	43.43 147.05	42	6.5 ISC
4 Oct. 25, 1965	22 h 34m 24.4 s	44.04°N 145.57°E	166km	
	22 34 24.7	43.73 145.52	160	JMA
	22 34 22.4	44.21 145.45	159	6.1 ISC
5 Nov. 15, 1961	7 h 17m 11.9 s	42.63°N 145.51°E	25km	
	7 17 09.9	42.65 145.57	60	6.9 JMA
6 June 11, 1965	3 h 33m 44.2 s	43.65°N 148.80°E	0km	6.4 JMA
	3 33 45.9	44.45 148.84	58	6.0 ISC

Parameters of no comments in the last column are determined by relocation.

seismograms and weighted according to their detection accuracies ; S arrivals were employed only for the first approximation to the origin time. The reference structure was K-4-A (KAKUTA, 1973) for events in the northeast but Jeffreys' model for event 2 in the southwest.

Seismograms on a record section were normalized in each figure to respective maximum amplitudes for comparing their waveforms.

### 3.1 The 1968 Tokachi-Oki Earthquake (Event 1)

Small amplitudes of the initial motions were characteristics of the 1968 Tokachi-Oki Earthquake with a JMA magnitude 7.9. In the seismograms bandpass filtered with cutoff frequencies of 0.05 and 0.5 Hz, isolated phases  $P_1$  to  $P_6$  were clearly discerned (Fig. 2). Since these phases were nearly equal in slowness, they were attributable to successive events occurring in a focal region.

Time lags from cross-correlations were systematically diverged for phases  $P_1$  and  $P_2$ , if we plotted them as a function of distance from the JMA epicenter : namely, the lags were rather high at stations of SAI, HMD, FKK and FKJ along the coast of the Japan Sea, and low

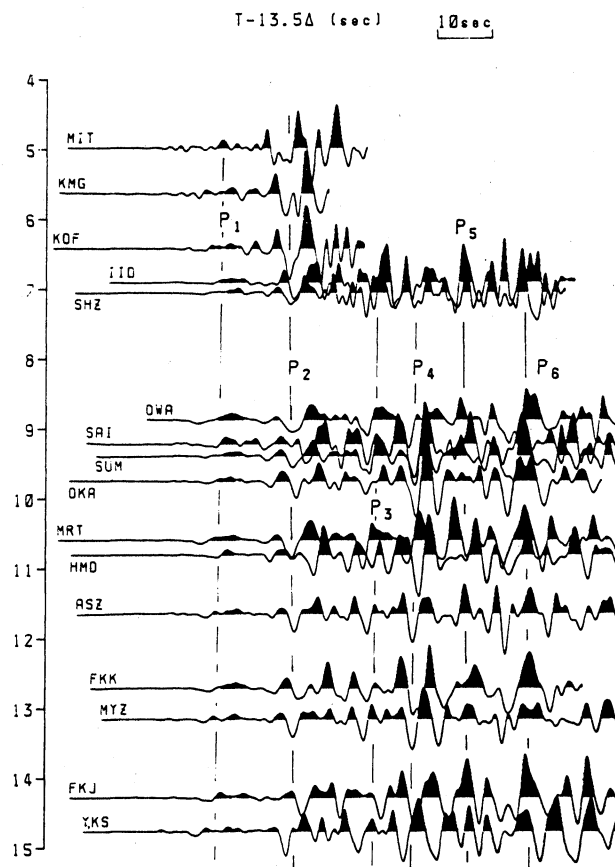


Fig. 2. Seismic record section for the 1968 Tokachi-oki earthquake (event 1) : vertical components filtered through a bandpass with cut-off frequencies of 0.05 and 0.5 Hz. All of seismograms are normalized to respective maximum amplitudes.

at OKA, MRT, ASZ, MYZ and YKS on the side of the Pacific coast (Fig. 3). A similar tendency was also discerned for other phases but less remarkable. Epicenters of  $P_1$  and  $P_2$  were consequently thought to be seriously separated from the JMA one.

A probable epicenter for each event was estimated on an assumption that time lags were linear as a function of distance in a limited range. The data were, however, insufficient for accurately locating events owing to stations distributed in a narrow azimuthal range. Starting from locations roughly approximated in a focal region of the large earthquake, we then iteratively estimated a few epicenters for an event. One of the epicenters which decreased the root mean square of residuals to a minimum largely diminished systematic deviations, as shown for  $P_2$ ,  $P_4$  and  $P_6$  in Fig. 4. Slownesses of six phases were 13.31-13.55 s/deg for the relocated epicenters, while 13.37-13.77 s/deg for the JMA epicenter [Table 2(a)]. If we excluded  $P_3$  and  $P_5$  less remarkable than others, the range was reduced to 13.40-13.50 s/deg. Its reciprocal of 8.2-8.3 km/s was very close to  $P_n$  velocity in the oceanic region.

Fig. 5 summarizes the epicenters together with those of other authors. Integer denotes each of  $P_1$  to  $P_6$ ;  $J$  refers to the JMA epicenter and  $N$  to the event of NAGAMUNE (1971);  $M$  and  $T$  stand for events of SCHWARTZ and RUFF (1985). The focal region is the aftershock area reproduced from the map of "Release of earthquake energy in and near Japan (1926-1974)" published by JMA. Considering the arrival times relative to the origin time, events  $P_2$  and  $P_6$  correspond to events  $M$  and  $T$  of SCHWARTZ and RUFF (1985) and  $P_4$  is the event related to the clear S phase of NAGAMUNE (1971). For all that our events were located far to the east of the corresponding ones, successive events  $P_2$  to  $P_6$  were roughly parallel to the direction of rupture estimated by SCHWARTZ and RUFF (1985).

Fig. 6 shows amplitude spectra and cross-spectra derived from records of 30 s in length

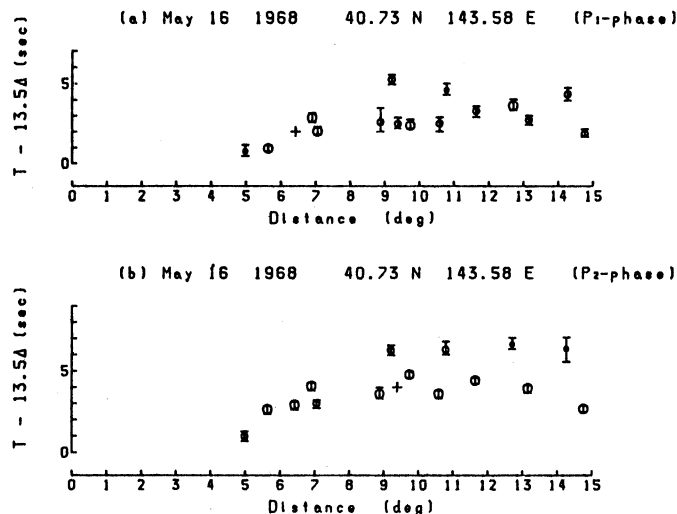


Fig. 3. Time lags derived from cross-correlations as a function of distance to the JMA epicenter of the 1968 Tokachi-oki earthquake : (a) event  $P_1$  (ref. KOF) and (b) event  $P_2$  (ref. SUM). Cross stands for the reference station and mark size shows the rank of time lag data.

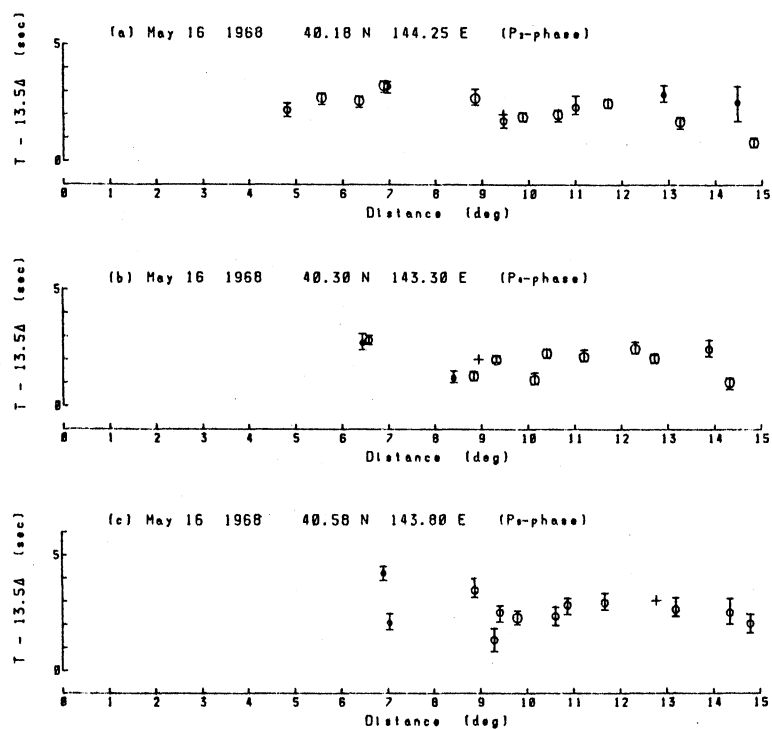


Fig. 4. Time lags derived from cross-correlations as a function of distance to relocated epicenters of the 1968 Tokachi-oki earthquake: (a)  $P_2$  (ref. SUM), (b)  $P_4$  (ref. SUM), and (c)  $P_6$  (ref. FKK). Note that systematic deviations of delays are largely diminished as compared with those in Fig. 3.

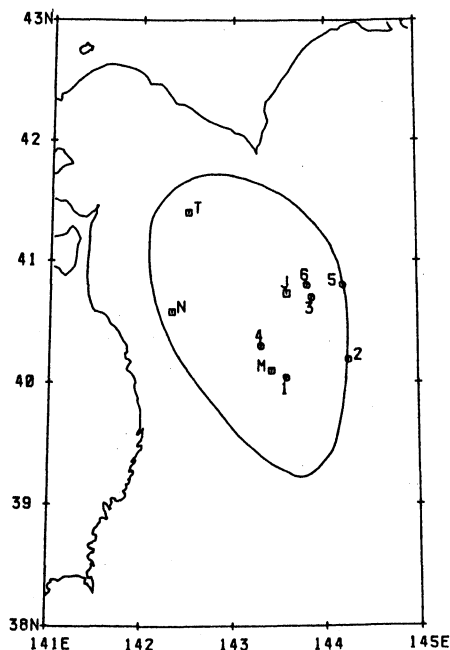


Fig. 5. Summary of various epicenters for the 1968 Tokachi-oki earthquake. Integers refer to events  $P_1$  to  $P_6$ .  $J$ : JMA.  $M$  and  $T$ : SCHWARTZ and RUFF (1985).  $N$ : NAGAMUNE (1971). The focal region is reproduced from the JMA map "Release of earthquake energy in and near Japan (1926-1974)".

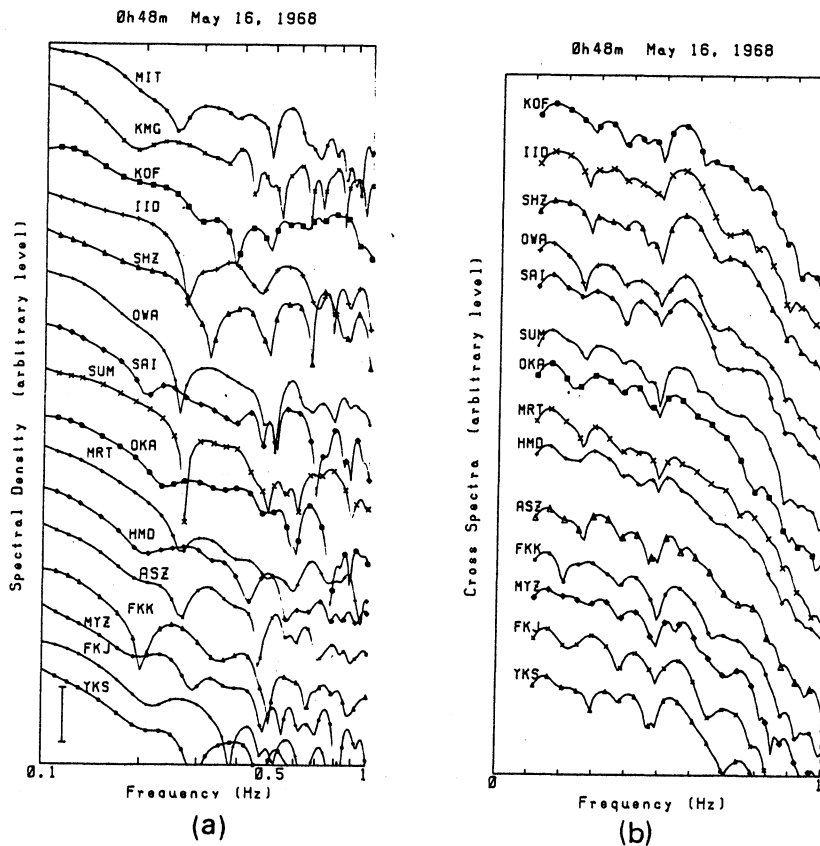


Fig. 6. Spectra of  $P_2$  derived from records of 30 s in length for the 1968 Tokachi-oki earthquake : (a) amplitude spectra and (b) cross-spectra (ref. MIT). Unit on a logarithmic scale is shown on the lower left.

including  $P_2$ . For spectral peaks as  $P_{F22}$  ( $0.308 \pm 0.016$  Hz),  $P_{F23}$  ( $0.410 \pm 0.007$  Hz) and  $P_{F24}$  ( $0.542 \pm 0.013$  Hz), slownesses were 13.28–13.30 s/deg (Fig. 7) rather lower than that estimated from cross-correlations for  $P_2$ . The epicenters decreasing residuals to a minimum were also different from that of  $P_2$ . These discrepancies were, however, probably insignificant owing to scattering of time lag data. Spectral peaks for  $P_4$  of large amplitude, such as  $P_{F42}$  ( $0.233 \pm 0.017$  Hz),  $P_{F43}$  ( $0.470 \pm 0.017$  Hz) and  $P_{F44}$  ( $0.590 \pm 0.011$  Hz), were not significantly different from  $P_4$  in slowness as well as in epicenter [Table 2(a)].

At a slowness of 13.40–13.50 s/deg appropriate to  $P_n$  phase, time lag curves for  $P_1$  to  $P_6$  extended linearly from  $4^\circ$  to  $15^\circ$  without any clear offsets. Standard deviations in slowness were appreciably less than those from travel times. Moreover, the results confirmed by several measurements will be more reliable than that by a single measurement. Correlation analysis of successive events occurring in a limited region was consequently very useful in slowness measurements.

### 3.2 The 1968 Hyuga-Nada Earthquake (Event 2)

Three phases of  $P_1$ ,  $P_2$  and  $P_3$  were detectable by visually correlating waveforms on a

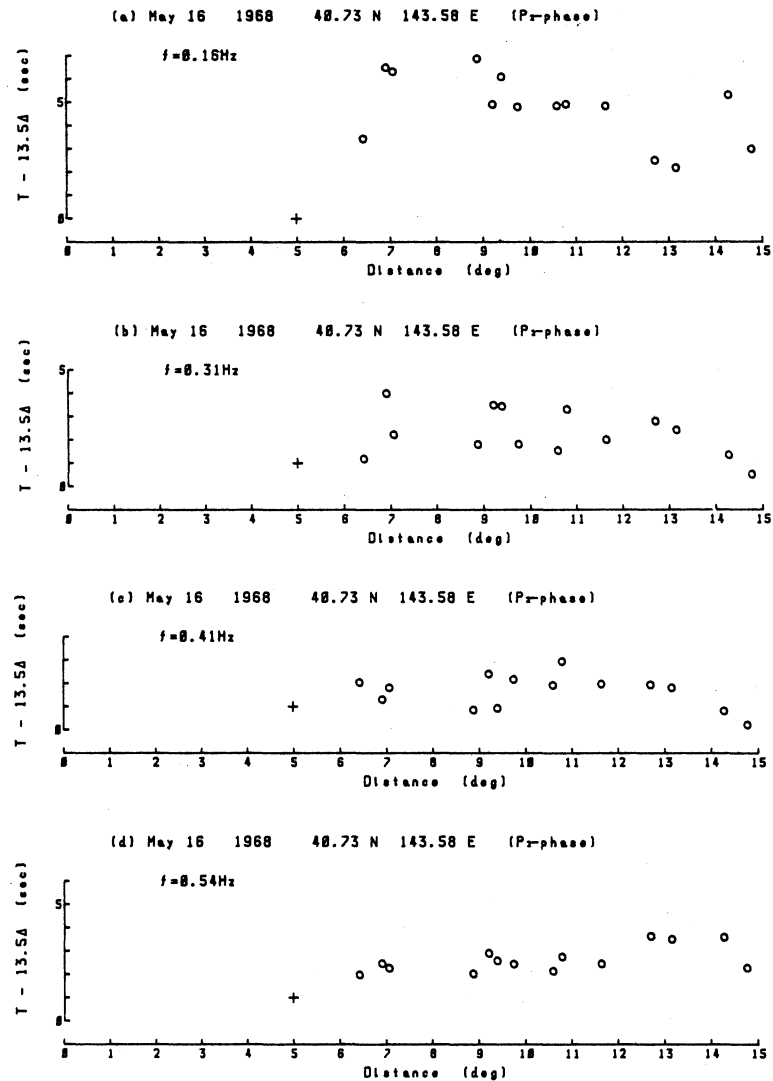


Fig. 7. Time lags versus distance to the JMA epicenter of the 1968 Tokachi-oki earthquake for spectral peaks of  $P_2$  in Fig. 6 (b) : (a)  $P_{F21}$ , (b)  $P_{F22}$ , (c)  $P_{F23}$ , and (d)  $P_{F24}$ . Mean frequency for each peak is given on the upper left.

record section of vertical component seismograms for the 1968 Hyuga-nada earthquake of a JMA magnitude 7.5 occurring in the uppermost mantle on the continental side of the Nankai trough (Fig. 8).

All the time lag curves as well as the travel time curve for the first arrival changed their respective slopes at about  $11^\circ$  as shown in Figs. 9 and 11. High slowness branches of 13.92-13.98 s/deg were reasonable, because they were consistent with  $P_n$  velocity (7.8-8.0 km/s) estimated from explosion seismic observations in southwest Japan (SASAKI *et al.*, 1970; IKAMI *et al.*, 1982; ITO *et al.*, 1982). Even very high slowness 15.10 s/deg for the most dominant spectral peak  $P_{F1}$  ( $0.190 \pm 0.010$  Hz) [Figs. 10 (b) and 11 (a), Table 2 (b)] was also comparable with the results of explosion seismic studies (HASHIZUME *et al.*, 1966; SASAKI *et al.*,

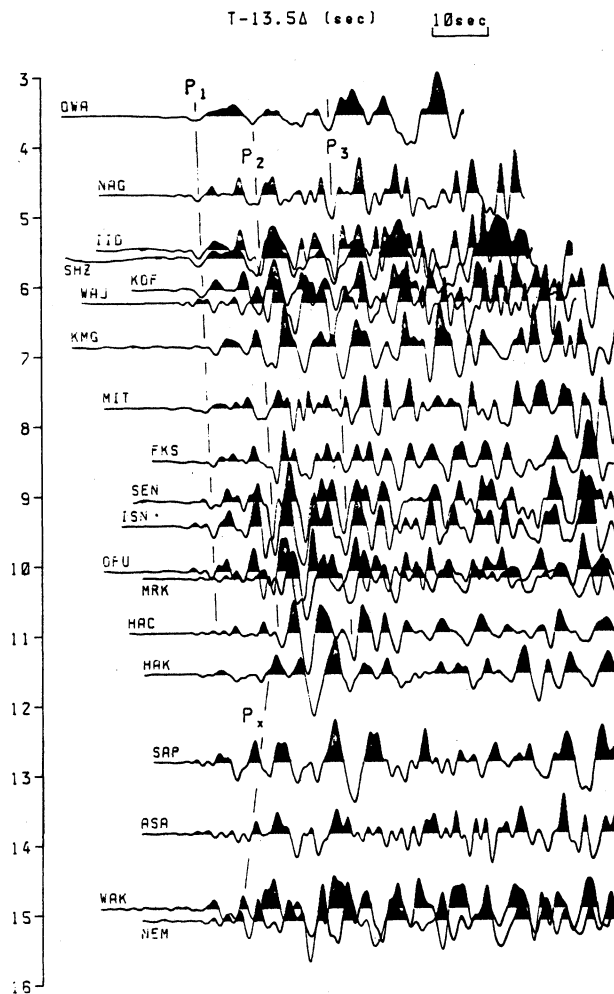


Fig. 8. Seismic record section for the 1968 Hyuga-nada earthquake (event 2) : vertical components bandpass filtered with cut-off frequencies of 0.05 and 0.5 Hz. All of seismograms are normalized to respective maximum amplitudes. Note a clear change in waveform at about 11°.

1970) : 7.4-7.6 km/s at depths of 30-50 km.

Slownesses were measured as 11.7-11.9 s/deg for low slowness branches of  $P_{X1}$  and  $P_{X2}$  in Fig. 9(b). They were also confirmed by that for spectral peak  $P_{FX}$  ( $0.190 \pm 0.010$  Hz) [Figs. 10(b) and 11(a) and Table 2(b)]. The branches of  $P_{X1}$  and  $P_{X2}$  were, however, probably not independent with each other but relevant to phase  $P_X$  (Fig. 8), considering the time difference of about 6 s between them. It was only a half of the difference between  $P_1$  and  $P_2$  and agreed well with the period of the dominant phase  $P_X$  (KAKUTA, 1978).

### 3.3 The 1964 East Off Hokkaido Earthquake (Event 3)

Two phases of P and  $P_1$  were visually traced on a record section for the 1964 East Off Hokkaido Earthquake of a JMA magnitude 6.7 (Fig. 12), regardless of small amplitude initial

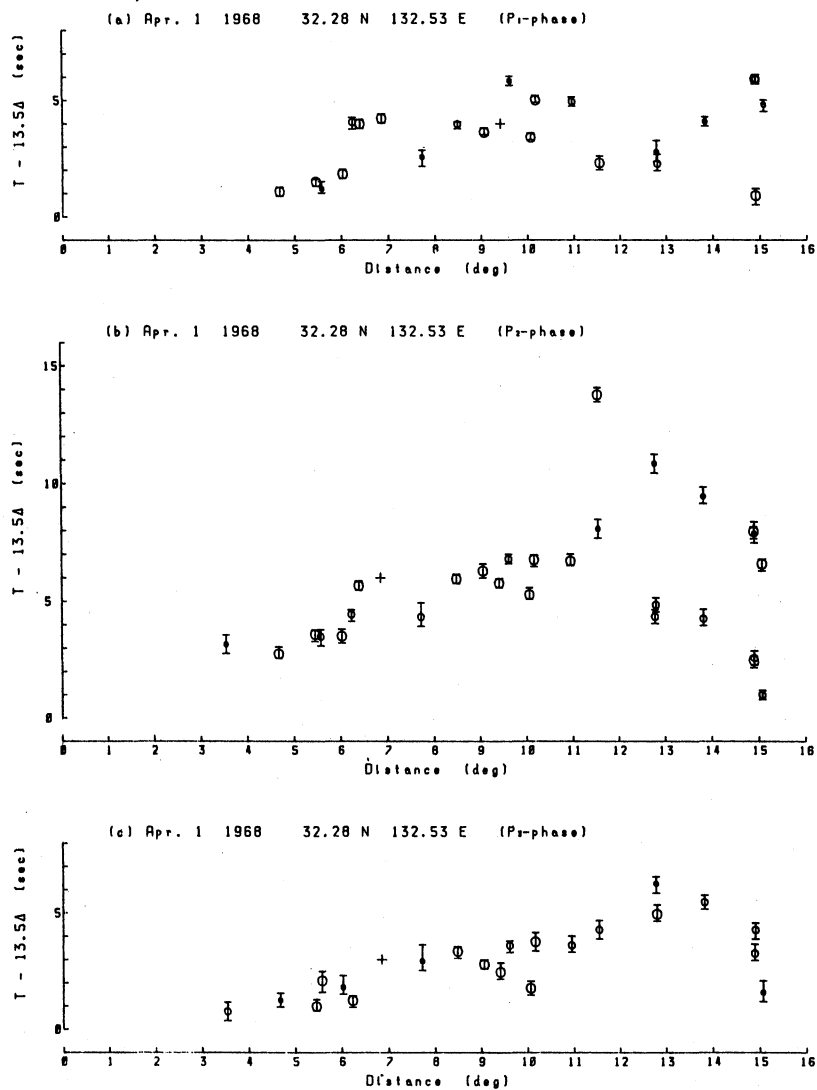


Fig. 9. Time lags versus distance to the JMA epicenter of the 1968 Hyuga-nada earthquake derived from cross-correlations : (a) P<sub>1</sub> (ref. ISN), (b) P<sub>2</sub> and P<sub>X</sub>'s (ref. KMG), and (c) P<sub>3</sub> (ref. KMG).

motions reversed between several stations : compressional at SEN, FKS, MIT, KMG, IID, KOC and ASZ and dilatational at MRK, ISN, KYO, SUM, HMD, FKK and NGS. At distances more than 13°, phase P almost disappeared and large amplitude phases P<sub>X1</sub> and P<sub>X2</sub> propagated at a low slowness of 11.99-12.20 s/deg [Figs. 13 (b) and (c)].

Phase P<sub>1</sub> followed P by about 15 s, which was nearly the same as the difference between P<sub>X1</sub> and P<sub>X2</sub>. Cross-correlations for P and P<sub>1</sub> gave their slownesses as 13.65-13.67 s/deg [Figs.13 (a) and (b)], which were also consistent with P<sub>n</sub> velocity in the region.

A low slowness of 11.36 s/deg was obtained for spectral peak P<sub>FX1</sub> (0.28 Hz) derived from seismic waves of 21 s long including P<sub>1</sub> in the central part. It were rather higher than that of 11.86 s/deg for P<sub>FX2</sub> (0.23 Hz) from those of 27 s long including phase P<sub>1</sub> in the first

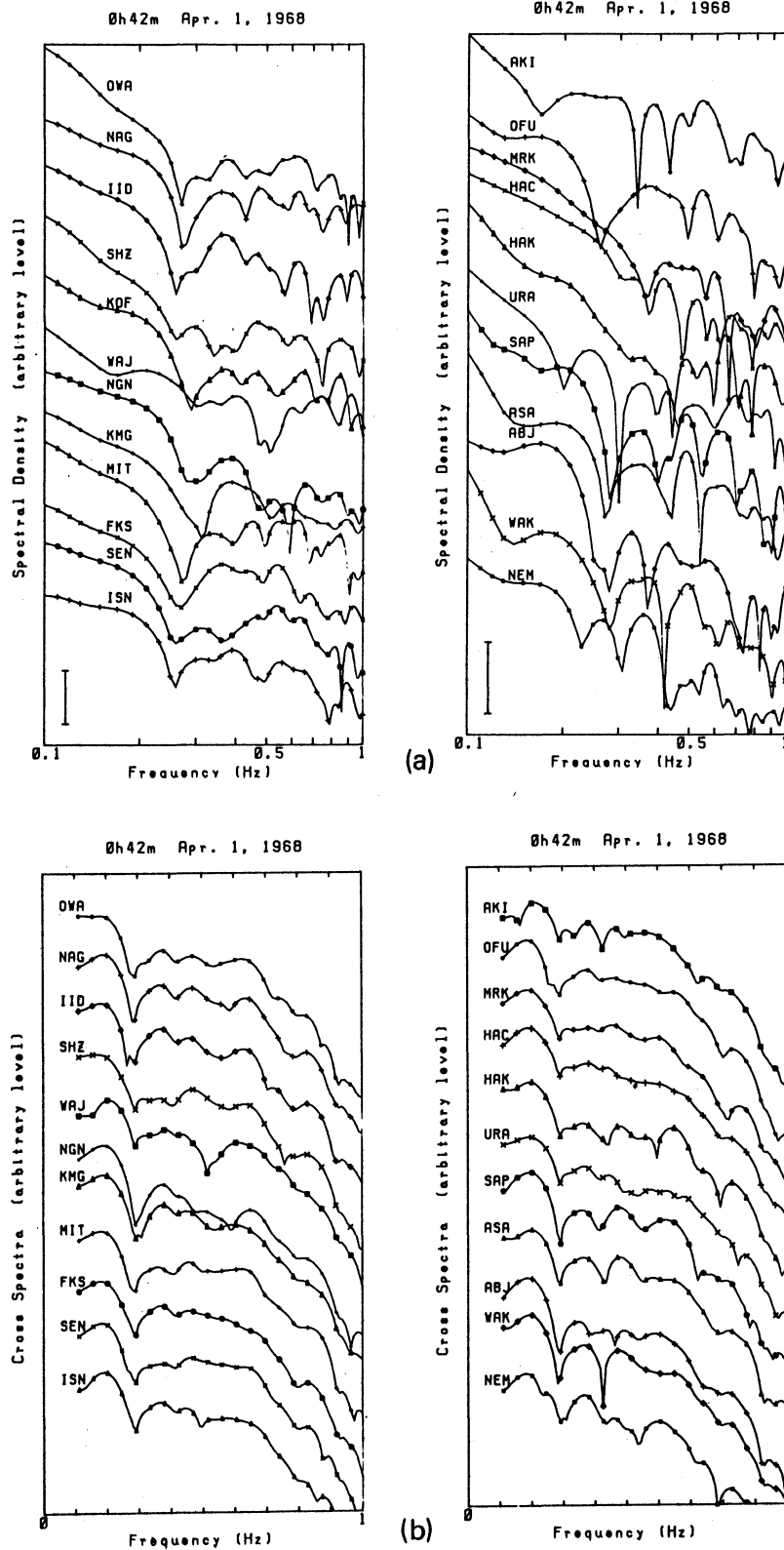


Fig. 10. Spectra of seismic waves of 30s in length containing both of  $P_1$  and  $P_2$  for the 1968 Hyuga-nada earthquake : (a) amplitude spectra and (b) cross-spectra (ref. KOF). Unit on a logarithmic scale is shown on the lower left.

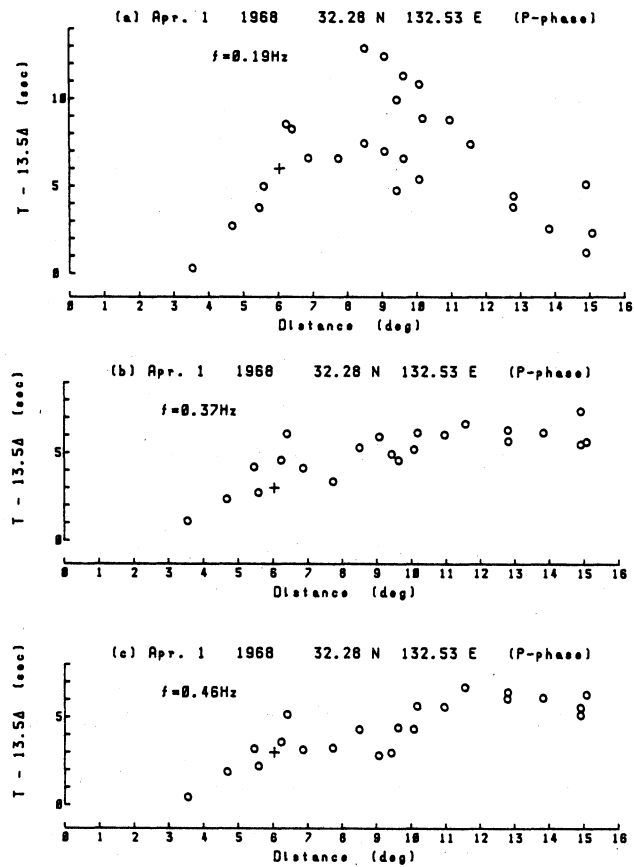


Fig. 11. Time lags versus distance to the JMA epicenter of the 1968 Hyuga-nada earthquake for spectral peaks in Fig. 10 (b) : (a)  $P_{F1}$  and  $P_{FX}$ , (b)  $P_{F2}$  and  $P_{FR2}$ , (c)  $P_{F3}$  and  $P_{FR3}$ . Mean frequency for each peak is given on the upper left.

half. An F-test with a significant level of 0.05, however, proved that both did not significantly differ from those for  $P_{X1}$  and  $P_{X2}$ . Table 2(c) summarizes slownesses; the epicenter in the last column was chosen out of JMA, ISC and relocated ones so that the standard deviation might be minimum in the measurement. Between slownesses for the three epicenters, differences were not larger than 0.08 s/deg.

### 3.4 The 1965 Kunashiri Island Earthquake (Event 4)

A relatively long-period P and an impulsive  $P_1$  were observed on a record section for an intermediate-depth earthquake occurring in the central part of Kunashiri Island (Fig.14). Slownesses from cross-correlations were 13.34 s/deg for P and for 13.16 s/deg for  $P_1$  [Figs. 15 (a) and (c)]. They agreed well with those for spectral peaks  $P_{F0}$  (0.30 Hz) and  $P_{F1}$  (0.46 Hz) derived from seismic waves containing both of P and  $P_1$  [Table 2(d)]. Phase  $P_1$  was traced up to about  $17^\circ$  on the time lag curve [Fig. 15(c)], while it was discernible to a distance less than  $13^\circ$  at the most on the section.

Large amplitude phase  $P_X$  of 11.87 s/deg [Fig. 15(d)] was very similar in slowness to

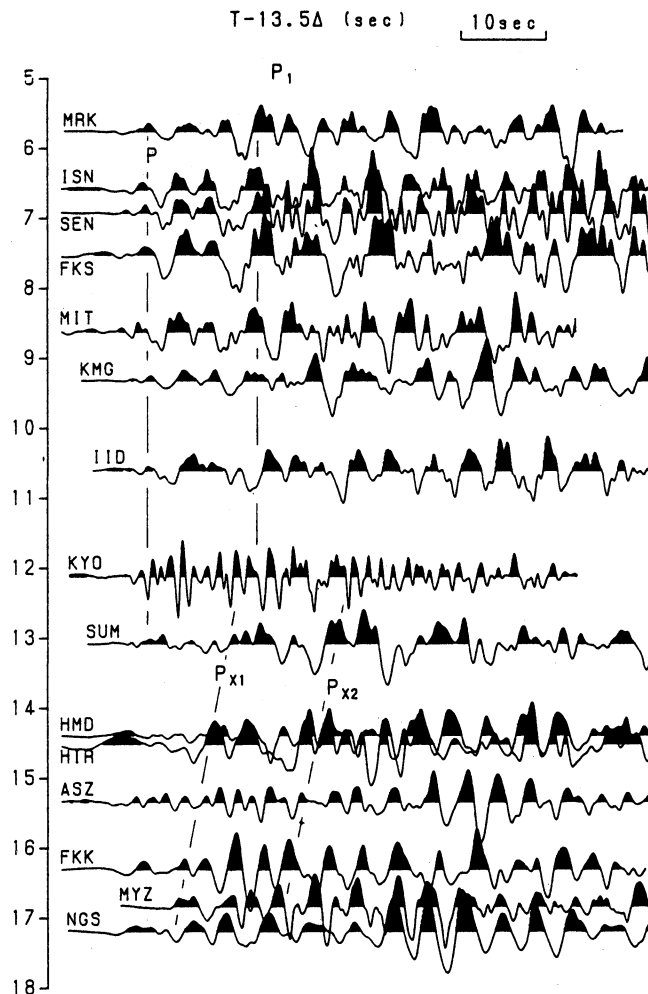


Fig. 12. Record section for the 1964 East Off Hokkaido earthquake (event 3) : vertical components except those of SUM, HIR and ASZ. Seismograms are corrected for instrumental response and bandpass filtered with cut-off frequencies of 0.1 and 1.0 Hz.

those for events 2 and 3. A dominant spectral peak  $P_{FX}$  (0.37 Hz) also confirmed the low slowness phase.

Correlating seismic waves including phase P with the reference of 13 s in length at IID, we detected phase  $P_R$  propagating at a low slowness of 12.52 s/deg [Figs.14 and 15(b)]. It was consistent with the slowness for  $P_{FR}$  (0.46 Hz). Such a phase was probably characteristic of intermediate depth earthquakes in the northeast region, since it had not been detected for any shallow events in the region.

### 3.5 The 1961 South Off Nemuro Earthquake (Event 5)

In spite of a shallow depth earthquake with a JMA magnitude 6.9, P onsets were clear at most Japanese stations on a record section (Fig. 16). Time lag curves for phase P by three methods extended almost linearly up to  $15^\circ$  at a slowness 13.4-13.5 s/deg quite consistent

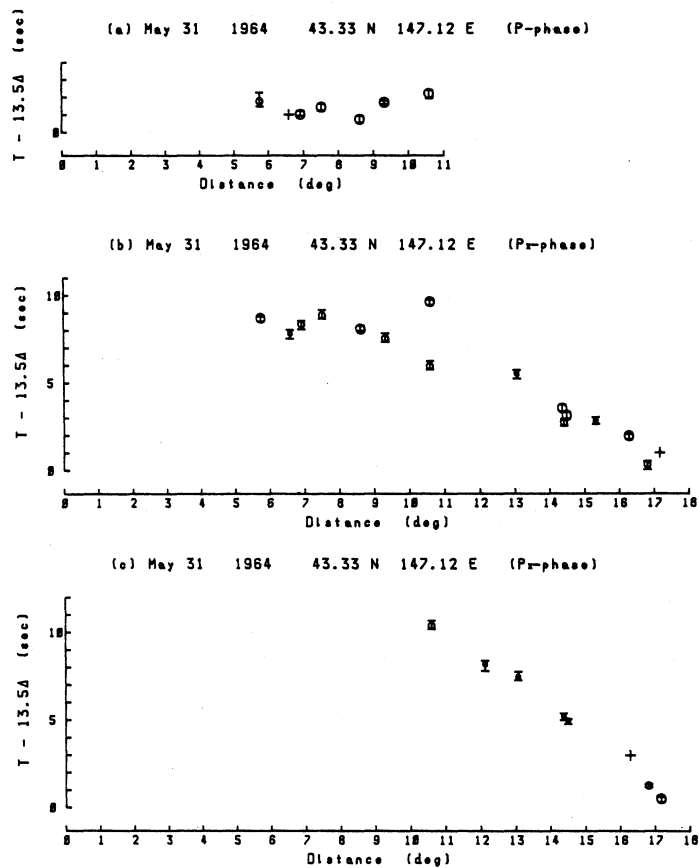


Fig. 13. Time lags derived from cross-correlations as a function of distance to the relocated epicenter of the 1964 East Off Hokkaido earthquake: (a) P (ref. ISN), (b)  $P_1$  and  $P_{X1}$  (ref. NGS), and (c)  $P_{X2}$  (ref. FKK). Cross refers to the reference station.

with  $P_n$  phase in the region [Table 2(e)]. They were very similar to the time curves for event 1 in slowness as well as in extending continuously to a greater distance. Such an aspect in the time curve was probably an important characteristic of time curves for earthquakes occurring at very shallow depths under the Pacific Ocean in the northeast region.

No phase except P could be related to  $P_n$  on the record section (Fig. 16). Phase  $P_x$  of 11.71 s/deg at distances more than  $9^\circ$  was therefore probably due to reflection (or refraction) of P; its slowness was confirmed by spectral peak  $P_{FX}$  (0.44 Hz). Branch  $P_x$  did not meet branch P at distances less than  $17-18^\circ$ , considering time differences between both phases.

### 3.6 The 1965 South Off Iturup Earthquake (Event 6)

Long-period arrivals P and  $P_1$  were discernible on a record section for an earthquake with a JMA magnitude of 6.4 (Fig. 17), although obscured and small-amplitude P waves were characteristics of seismograms at Japanese stations. This earthquake had been

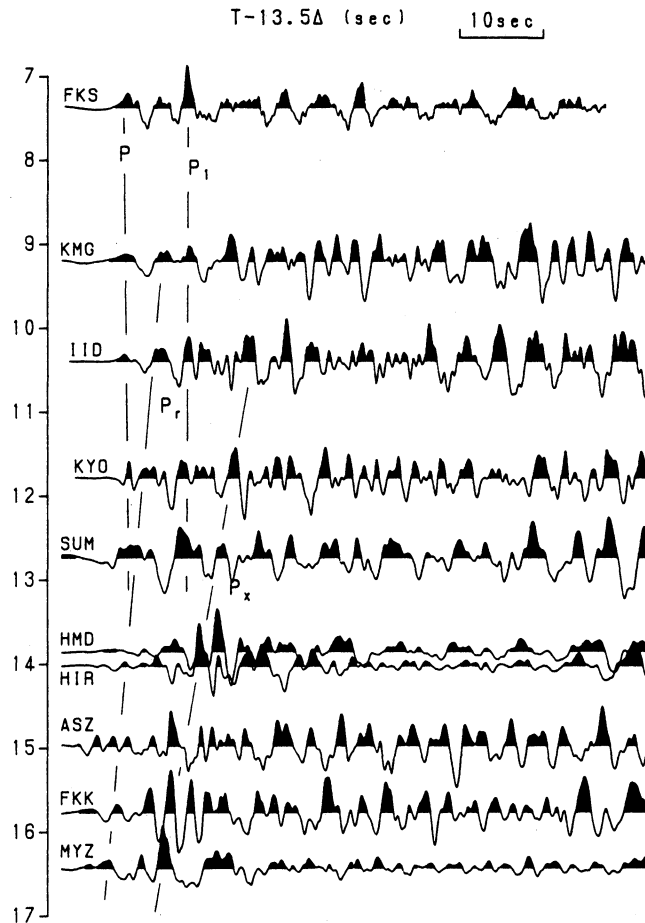


Fig. 14. Record section for the 1965 Kunashiri Island earthquake (event 4) : vertical components except those of ASZ and FKK. Seismograms are corrected for instrumental response and bandpass filtered with cut-off frequencies of 0.15 and 1.5 Hz.

located by JMA at a very shallow depth, which agreed well with a supplementary estimation of ISC. Cross-correlations for  $P$  and  $P_1$  gave their slownesses as 13.42-13.58 s/deg corresponding to  $P_n$  phase in the region. They were consistent with those of three spectral peaks  $P_{F11}$  (0.18 Hz),  $P_{F12}$  (0.34 Hz) and  $P_{F13}$  (0.47 Hz) for  $P$  as well as two peaks  $P_{F21}$  (0.22 Hz) and  $P_{F22}$  (0.43 Hz) for  $P_1$  [Table 2(f)]. Most of the time lag curves extended linearly without clear discontinuities in slope as easily seen in the record section (Fig. 17). Not only branches continuous up to  $18^\circ$  but also slownesses fit for  $P_n$  phase were comparable with the time curves for other earthquakes of very shallow focal depth.

Regardless that cross-correlations were not useful to detect low slowness phase  $P_x$  owing to low coherence, spectral peak  $P_{Fx}$  (0.34 Hz) of 11.67 s/deg was consistent with  $P_x$ 's from other events.

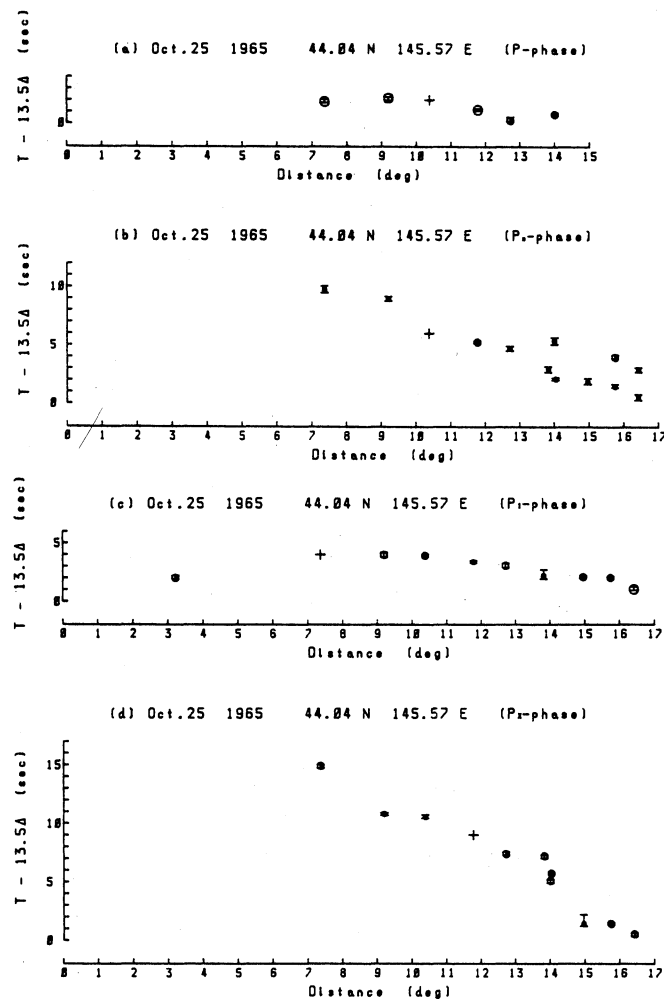


Fig. 15. Time lags derived from cross-correlations as a function of distance to the relocated epicenter of the 1965 Kunashiri Island earthquake: (a) P (ref. IID), (b) P<sub>r</sub> (ref. IID), (c) P<sub>1</sub> (ref. FKS) and (d) P<sub>x</sub> (ref. KYO).

#### 4. Record Section for S Waves

Waveforms changed greatly from station to station on record sections of NS and EW components of S seismograms. Consequently, high correlations were not available over a distance range wide enough to measure a slowness accurately even on a record section of rotated seismograms filtered through a bandpass. The incoherence in the S seismograms was probably owing to nonlinear ground motions (NUTTLI, 1961) and/or to mixing of several phases at various slownesses.

We used record sections of NS and EW components to display S phases for events 3 and 4, because cross-correlations were not effective in analyzing S waves. Arrival times were detected on the sections, while cross-spectra were computed from radial and transverse components.

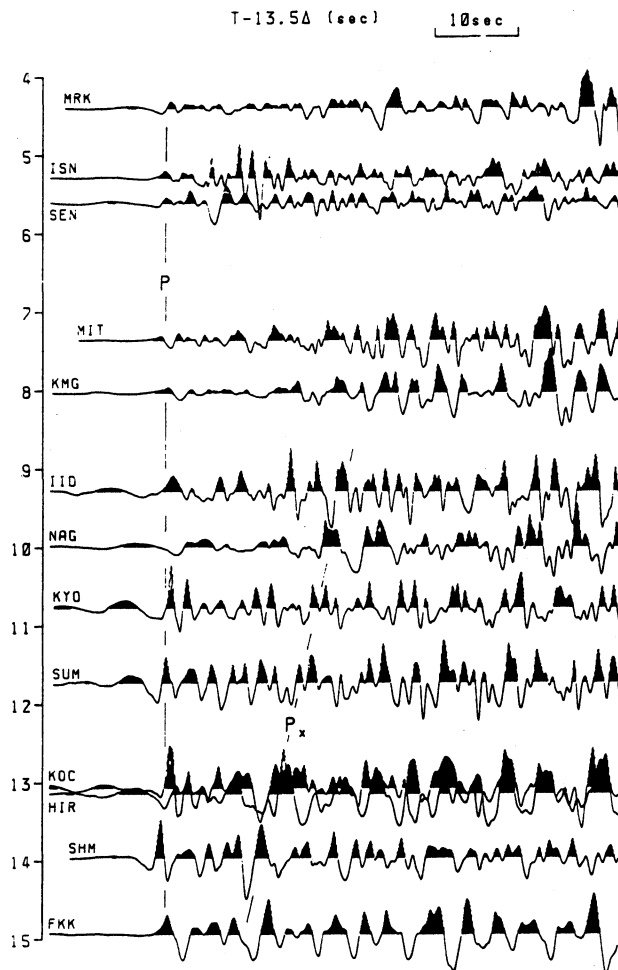


Fig. 16. Record section for the 1961 South Off Nemuro earthquake (event 5) : vertical components except that of SUM. Seismograms are corrected for instrumental response and bandpass filtered with cut-off frequencies of 0.15 and 1.5 Hz.

#### 4.1. Seismograms of Event 3

Three arrivals were detected in record sections of NS and EW components of S seismograms sampled at intervals of 0.2 s for the 1964 East Off Hokkaido earthquake : the first S of slowness 23.7 s/deg, a large amplitude phase,  $S_1$ , following the first S by about 15 s, and a large later arrival,  $S_x$ , of long-period (Fig. 18). At MIT, KMG, IID and KYO, onsets of the first S of relatively large amplitude were clear in the seismograms dominated with short-period waves, while they appeared at 10-15 s earlier than the theoretical times for Jeffreys-Bullen model. The first S as well as short-period waves was highly attenuated at 14° or more. The long-period phase dominated at a low slowness instead. Such a great change in waveform near 13° had been observed on the record section for P waves in Fig. 12.

From about 80 s of record length including both of S and  $S_1$ , slownesses were estimated as 24.3-24.5 s/deg for two peaks at 0.23 Hz and 0.27 Hz for the transverse component and a peak at 0.32 Hz for the radial component. They were 1.78-1.80 times as large as the

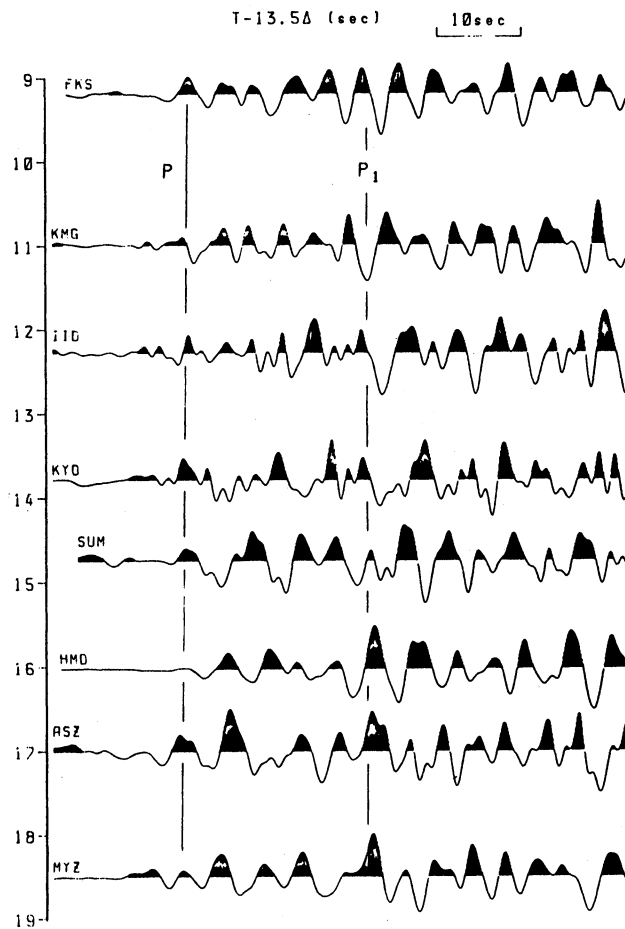


Fig. 17. Record section for the 1965 South Off Iturup earthquake (event 6) : vertical components corrected for instrumental response and bandpass filtered with cut-off frequencies of 0.05 and 0.5 Hz.

slownesses for  $P$  and  $P_1$  [Table 2(c)] : UTSU (1969) estimated the  $V_P/V_S$  ratio as 1.77 for the upper mantle in the Japan region. Since the slowness ratio of the first S to P was 1.73, the slowness derived from arrival times of the first S was also not significantly different from them. A peak at 0.11 Hz for the transverse component also confirmed the estimation for the first S.

A weak arrival, which was found at MYZ and NGS at 14-16 s later than the expected time for the first S, was likely to belong to branch  $S_1$ . The time difference of 15 s between S and  $S_1$  was nearly equal to that between P and  $P_1$ . Namely, the 15s-later arrivals were found not only in S waves but also in P waves for this earthquake. These facts strongly suggested that  $S_1$  was an S phase closely related to  $P_1$ .

Long-period later phase  $S_x$  dominating at distances more than  $12^\circ$  probably corresponded to  $P_x$ .

## 4.2 Seismograms of Event 4

Waveforms in record sections of S seismograms, which were sampled at 0.1 s, changed their aspects clearly near  $13^\circ$  for the 1965 Kunashiri earthquake (Fig. 19) as those did in the P seismograms (Fig. 14). At  $13^\circ$  or more, short period waves were attenuated and later phase  $S_x$  dominated. A discontinuity near  $13^\circ$  was also observed in a time lag curve for a low frequency peak at 0.09 Hz derived from transverse components of 40 s in record length. If we referred to K-4-A under the assumption of  $V_P/V_S$  1.77, a time gap of 8-9 s should be observed at  $12.4^\circ$  in the time curve for the first S. The first S of 23.4 s/deg was, however, traced up to  $16.4^\circ$  on the section. Its slowness was quite well consistent with those of

Table 2. P wave slowness estimated from three types of data :

(1) travel times, (2) time lags from cross-correlations and (3) time lags from cross-spectra. Epicenter in the last column is chosen out of ISC, JMA and relocated ones so that the standard deviation is minimum in the measurement. Except the largest earthquake (event 1), variance in epicenter did not produce differences greater than 0.10 s/deg in estimation of slowness.

(a) the 1968 Tokachi-Oki Earthquake (event 1)

		slowness ( $dT/d\Delta$ )	distance range	epicenter	
		(s/deg)	(deg)		
(1)	P	$13.855 \pm 0.171$	4.99 - 14.77	$40.73^\circ N$	$143.58^\circ E$ (JMA)
(2)	$P_1$	13.420 0.044	4.40 14.33	40.04	143.58
	$P_2$	13.402 0.045	4.83 14.83	40.19	144.26
	$P_3$	13.309 0.051	7.02 14.90	40.70	143.85
	$P_4$	13.442 0.068	6.44 14.33	40.30	143.30
	$P_5$	13.564 0.081	7.28 15.17	40.80	144.19
	$P_6$	13.496 0.076	7.07 14.94	40.80	143.80
(3)	$P_{F21}$	13.041 0.113	6.90 14.76	40.73	143.58 (JMA)
	$P_{F22}$	13.275 0.070	5.34 15.23	40.80	144.30
	$P_{F23}$	13.299 0.050	5.33 15.22	40.81	144.27
	$P_{F24}$	13.288 0.040	4.79 14.66	40.45	143.70
	$P_{F41}$	13.706 0.101	9.17 15.10	40.66	144.22
	$P_{F42}$	13.525 0.120	6.44 14.33	40.30	143.30
	$P_{F43}$	13.359 0.038	6.44 14.33	40.30	143.30
	$P_{F44}$	13.405 0.077	6.44 14.33	40.30	143.30

## (b) the 1968 Hyuga-Nada Earthquake (event 2)

		slowness ( $dT/d\Delta$ )	distance range		epicenter		
		(s/deg)	(deg)				
(1)	P	$14.030 \pm 0.127$	3.55–10.18		$32.28^\circ\text{N}$	$132.53^\circ\text{E}$	(JMA)
	P <sub>r</sub>	12.774 0.073	10.94	15.07	32.48	132.28	(ISC)
(2)	P <sub>1</sub>	13.969 0.108	4.77	11.08	32.08	132.60	
	P <sub>2</sub>	13.976 0.080	3.46	10.91	32.22	132.71	
	P <sub>3</sub>	13.920 0.064	3.38	11.36	32.45	132.65	
	P <sub>X1</sub>	11.910 0.202	11.55	15.06	32.20	132.70	
	P <sub>X2</sub>	11.697 0.116	11.67	15.17	32.10	132.63	
(3)	P <sub>F1</sub>	15.101 0.225	3.55	7.74	32.28	132.53	(JMA)
	P <sub>F2</sub>	13.996 0.075	3.46	10.91	32.22	132.71	
	P <sub>F3</sub>	13.907 0.078	3.61	11.08	32.08	132.63	
	P <sub>FX</sub>	11.854 0.103	8.53	15.07	32.48	132.28	(ISC)
	P <sub>Fr2</sub>	13.228 0.082	11.51	15.05	32.38	132.46	
	P <sub>Fr3</sub>	13.067 0.048	11.66	15.04	32.10	132.63	

## (c) the 1964 East Off Hokkaido Earthquake (event 3)

		slowness ( $dT/d\Delta$ )	distance range		epicenter		
		(s/deg)	(deg)				
(1)	P	$13.690 \pm 0.166$	5.79–10.62		$43.27^\circ\text{N}$	$147.23^\circ\text{E}$	(JMA)
	P <sub>r</sub>	13.054 0.154	11.36	17.20	43.43	147.05	(ISC)
(2)	P	13.671 0.088	5.79	10.62	43.27	147.23	(JMA)
	P <sub>1</sub>	13.649 0.148	5.79	10.62	43.27	147.23	(JMA)
	P <sub>X1</sub>	12.197 0.113	10.64	17.20	43.43	147.05	(ISC)
	P <sub>X2</sub>	11.993 0.059	10.62	17.23	43.27	147.23	(JMA)
(3)	P <sub>F1</sub>	14.118 0.069	5.78	13.10	43.43	147.05	(ISC)
	P <sub>FX1</sub>	11.357 0.104	14.43	17.23	43.27	147.23	(JMA)
	P <sub>F2</sub>	13.364 0.063	5.78	13.10	43.43	147.05	(ISC)
	P <sub>FX2</sub>	11.855 0.197	12.14	17.20	43.43	147.05	(ISC)

## (d) the 1965 Kunashiri Island Earthquake (event 4)

		slowness ( $dT/d\Delta$ )	distance range	epicenter		
		(s/deg)	(deg)			
(1)	P	$13.153 \pm 0.088$	7.37–14.02	44.04°N	145.57°E	
(2)	P	13.338 0.081	7.46 14.06	44.21	145.45	(ISC)
	P <sub>r</sub>	12.516 0.060	7.46 16.48	44.21	145.45	(ISC)
	P <sub>1</sub>	13.160 0.041	7.37 16.43	44.04	145.57	
	P <sub>x</sub>	11.868 0.115	7.09 16.19	43.73	145.52	(JMA)
(3)	P <sub>F0</sub>	13.429 0.042	7.09 11.53	43.73	145.52	(JMA)
	P <sub>F1</sub>	13.485 0.109	7.09 11.53	43.73	145.52	(JMA)
	P <sub>Fr</sub>	12.477 0.105	11.84 16.48	44.21	145.45	(ISC)
	P <sub>Fx</sub>	11.470 0.162	10.12 16.19	43.73	145.52	(JMA)

## (e) the 1961 South Off Nemuro Earthquake (event 5)

		slowness ( $dT/d\Delta$ )	distance range	epicenter		
		(s/deg)	(deg)			
(1)	P	$13.471 \pm 0.080$	4.40–14.93	42.65°N	145.57°E	(JMA)
(2)	P	13.485 0.057	4.44 14.98	42.63	145.51	
	P <sub>x</sub>	11.713 0.158	9.32 14.98	42.63	145.51	
(3)	P <sub>F1</sub>	13.384 0.056	4.40 14.93	42.65	145.57	(JMA)
	P <sub>F2</sub>	13.496 0.036	4.44 14.98	42.63	145.51	
	P <sub>FX</sub>	11.475 0.162	9.32 14.98	42.63	145.51	

23.4–23.9 s/deg estimated for three spectral peaks at 0.18 Hz, 0.26 Hz and 0.43 Hz from radial components of 33 s in length. Its arrival times were only 2–3 s earlier at some stations (IID, KYO, SUM and ASZ) than the theoretical times for Jeffreys-Bullen model. It was hence considered that the first S was accurately traced.

A slowness appropriate to S<sub>x</sub> was measured as 21.1 s/deg for a low frequency peak at 0.09 Hz from transverse components. Considering the ratio of  $V_P/V_S$ , S<sub>x</sub> was probably related to P<sub>x</sub>. On the other hand, 22.3 s/deg for a high frequency peak at 0.43 Hz from radial components possibly corresponded to an S phase associated with P<sub>r</sub>.

(f) the 1965 South Off Iturup Earthquake (event 6)

		slowness ( $dT/d\Delta$ )	distance range	epicenter		
		(s/deg)	(deg)			
(1)	P	$13.678 \pm 0.160$	9.19–18.50	44.45°N	148.84°E	(ISC)
(2)	P	13.419 0.112	8.64 18.00	43.65	148.80	(JMA)
	$P_1$	13.580 0.063	8.64 18.00	43.65	148.80	(JMA)
(3)	$P_{F11}$	13.183 0.132	9.19 18.50	44.45	148.84	(ISC)
	$P_{F12}$	13.256 0.048	8.64 18.00	43.65	148.80	(JMA)
	$P_{F13}$	13.303 0.086	9.19 18.50	44.45	148.84	(ISC)
	$P_{FX}$	11.666 0.055	14.76 18.50	44.45	148.84	(ISC)
	$P_{F21}$	13.547 0.060	9.19 18.50	44.45	148.84	(ISC)
	$P_{F22}$	13.357 0.043	9.19 18.50	44.45	148.84	(ISC)

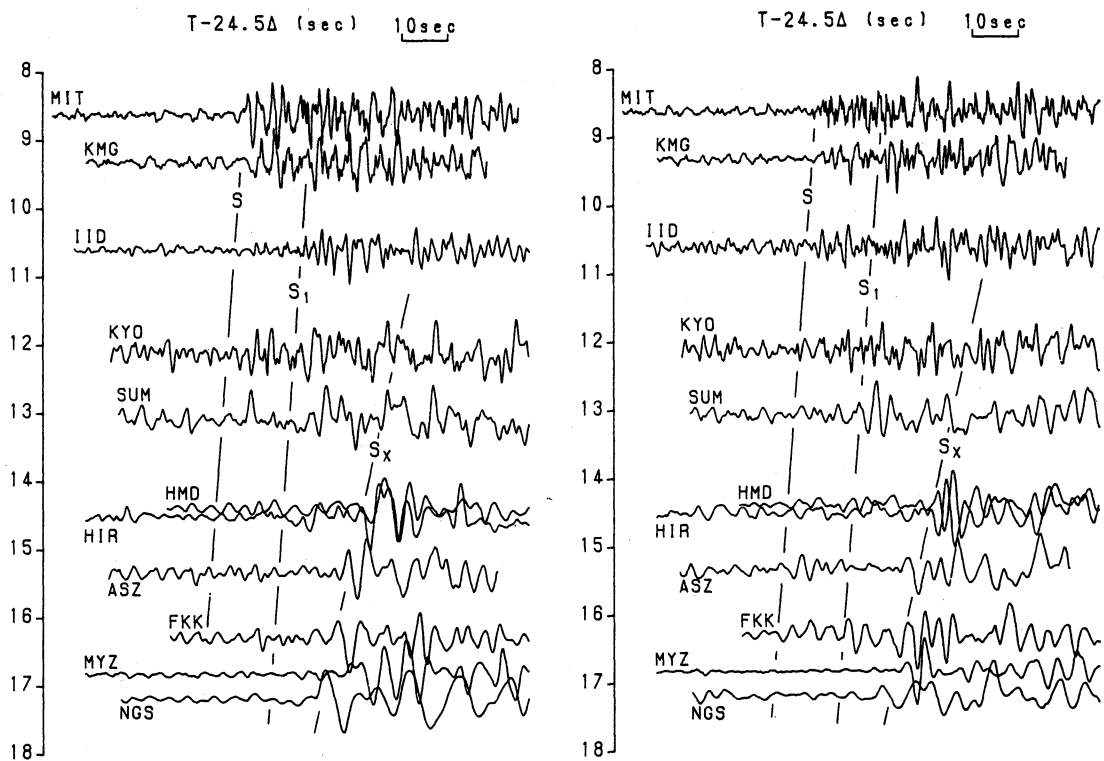


Fig. 18. S record sections for the 1964 East Off Hokkaido earthquake (event 3) : NS component on the left and EW one on the right. All of seismograms are normalized to respective maximum amplitudes. Note the first S apparently disappearing at 16-17°.

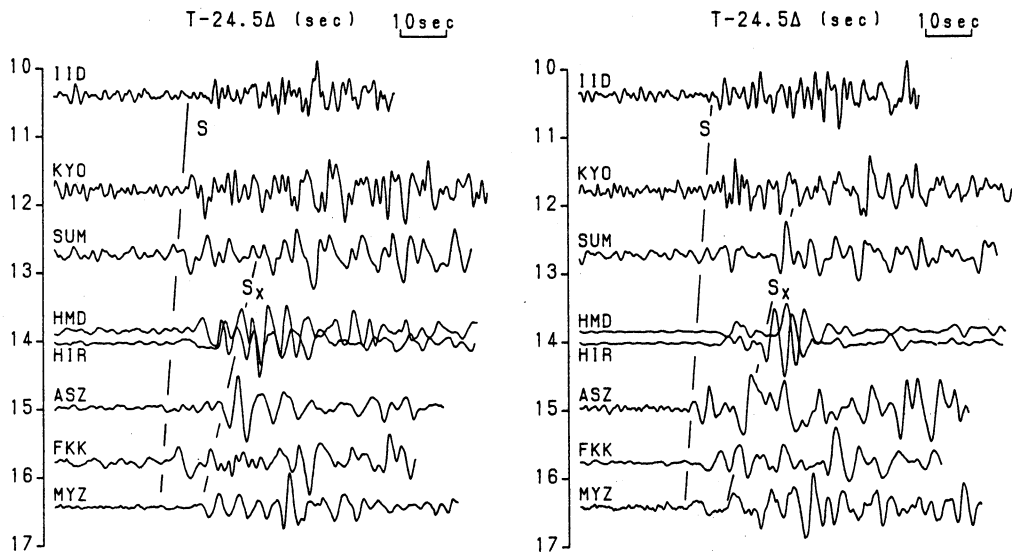


Fig. 19. S record sections for the 1965 Kunashiri Island earthquake (event 4) : NS component on the left and EW one on the right.

### 5. Low Velocity Layer in the Upper Mantle

The transition from  $P_n$  to  $P_x$  for event 2 occurred at about  $11^\circ$  as if it were associated with  $13^\circ$ -discontinuity (the low velocity layer). Such a change was also evident in amplitude spectra of seismic waves of about 30 s in length containing  $P_1$  and  $P_2$  [Fig. 10 (a)]. Namely, peaks at about 0.20 Hz and at 0.3–0.4 Hz were clear at large distances (SAP, ASA, ABJ and WAK), while they were obscured within  $10^\circ$ ; a trough at about 0.3 Hz was not discernible at the stations near  $11^\circ$  (MRK, HAC and HAK). Remarkable changes also occurred at  $11$ – $13^\circ$  for event 3 in waveform on the record section and in slope of the time lag curve (Figs. 12 and 13).

The slowness for  $P_x$  was, however, noticeably lower than that theoretically expected for P waves refracted from the base of the low velocity layer. Besides, no clear caustic was found on the record section. An apparent offset was surely noticed near  $16^\circ$  in S waves for event 3 (Fig. 18); instead of the first S fading out, an apparent delayed S was detected at MYZ and NGS. Nevertheless, the delayed S phase was not ascribed to the low velocity layer, because its corresponding P phase, or  $P_1$  (Fig. 12), had been interpreted as caused by one other event.

Fig. 20 shows the amplitude spectral density of a peak in the frequency range, which is shown in the top of respective figures, for events 2 and 3 as a function of distance, together with geometrical spreading curves on the assumption of Jeffreys' model and  $Q_p$  of 100. At a few stations near  $14^\circ$ , amplitudes were four times as large as the theoretical decaying curve for event 3 [Fig. 20 (b)]. Such an increase in amplitude can, however, be explained from the focal mechanism and is not necessarily ascribed to the low velocity layer.

Time lag curves corresponding to  $P_n$  phase were almost continuous from  $5^\circ$  to  $15$ – $18^\circ$  for

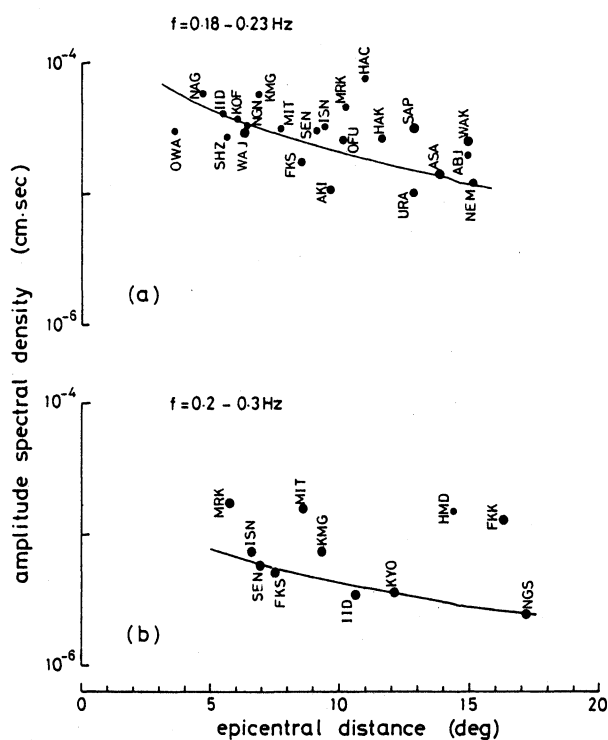


Fig. 20. Amplitude spectral density versus distance for P waves : (a) event 2 and (b) event 3. When spectral peak is not found in the frequency range on the upper left in each figure, the maximum is shown by small circle. Solid line shows a geometrical spreading curve for Jeffreys' model with  $Q_P=100$ .

very shallow earthquakes as events 1, 5 and 6. They were surprisingly simple in comparison with the time curve of ARC-TR (FUKAO, 1977) including a low velocity layer at depths from 85 to 165 km. On the record sections, neither a caustic near  $12^\circ$  nor a time gap of about 4 s was discernible, although they were expected from ARC-TR.

As the evidence for the low velocity layer in the upper mantle, KANAMORI (1967) pointed out that the first P arrival of small amplitude was followed by a strong later phase appearing several seconds late at  $14^\circ$ . There are many reports of weak first arrivals followed by a strong later phase near  $14^\circ$  — GUTENBERG (1948), KISHIMOTO and KAMITSUKI (1957), JOHNSON (1967), ARCHAMBEAU *et al.* (1969), HELMBERGER and WIGGINS (1971), DRUMMOND *et al.* (1982), for example. Most of the authors ascribed such amplitude behavior to the low velocity layer, while few reports have presented clear observations of the shadow zone attributable to it. KISHIMOTO and KAMITSUKI (1957) doubted the existence of the layer in the Japan region because the branch of direct waves with small amplitude was continued up to  $18^\circ$  in their study.

A rapid decrease or increase in amplitude was not confirmed in the observed decaying curves and time gaps ascribable to a low velocity layer was not noticed on the record sections. These facts will probably be explained by a low- $V$  zone under the lithosphere :

its upper surface is dipping and convexly curving. The dipping boundaries convexly curving may diverge seismic rays and then do not produce any caustics. Furthermore, several ray paths possibly satisfy the principle of stationary time in a structure laterally varying. A rapid decrease or increase in amplitude as well as a time gap will consequently be obscured. According to KAKUTA (1973), a velocity structure similar to the above model explained well P travel time anomalies for the earthquakes occurring at shallow and intermediate depths in the Kuril-Hokkaido-Northeast Japan arc.

## 6. Discussion

Fig. 21 summarizes P slownesses for events 2, 3 and 4 together with theoretical curves, which refer to Jeffreys' model for event 2 and to K-4-A (KAKUTA, 1973) for events 3 and 4.

Jeffreys' model explained well the slownesses of 13.9-14.0 s/deg consistent with  $P_n$  velocities in the southwest region but did not abruptly change in slowness at about  $11^\circ$  [Fig. 21(a)]. For events 3 and 4, K-4-A was fit for the observations at shorter distances; namely, 13.30-13.69 s/deg for event 3 [Fig. 21(b)] corresponded to theoretical slownesses decreasing from 13.7 s/deg at  $5^\circ$  to 13.0 s/deg at  $18^\circ$  and 13.16-13.34 s/deg for event 4 [Fig. 21(c)] to those from 13.2 s/deg at  $7^\circ$  to 13.0 s/deg at  $14^\circ$ . Low slowness phase  $P_x$  of large amplitude may be attributable to a reflection at such a sharp discontinuity in the upper mantle as  $13^\circ$ - or  $20^\circ$ -discontinuity because its slowness was substantially independent of focal depth. Nevertheless, it was not sufficiently explained by K-4-A or Jeffreys' model.

For the events in the northeast region, the  $13^\circ$ -discontinuity could not explain that  $P_n$  phase was observable up to  $17$ - $18^\circ$  for very shallow earthquakes (Figs. 16 and 17). Besides, the slowness of 11.5-12.0 s/deg was excessively low for a phase related to the discontinuity. Its apparent velocity, 9.2-9.7 km/s, was comparable with that of a phase reflected at a sharp discontinuity near 400 km deep as reported by FUKAO (1977). Then  $P_x$  was probably ascribable to the  $20^\circ$ -discontinuity.

On the other hand, phase  $P_x$  for event 2 could not be explained similarly. In spite of the focal depth being shallow, the time lag curve changed abruptly its slope near  $11^\circ$ . The change occurred at a distance closely related to  $13^\circ$ -discontinuity. The phase  $P_x$  accordingly seemed as if it were refracted from a zone immediately underlying the low velocity layer (JOHNSON, 1967; KANAMORI, 1967; FUKAO, 1977). Its apparent velocity was, however, too high for a discontinuity at about 200 km. In our interpretation, it was a phase reflected at about 200 km deep but not ascribed to  $13^\circ$ -discontinuity; the high apparent velocity was due to the discontinuity inclined to the southwest or to the west. Such a discontinuity surely corresponds to the upper boundary of the lithosphere in northeast Japan; an example had been shown for a theoretical ray reflected at the boundary in Fig. 14(b) of KAKUTA (1985).

In the northeast region,  $P_r$  of 12.5 s/deg was observed only for event 4 of intermediate depth. Its slowness was certainly fit for a phase refracted from a zone immediately underlying the low velocity layer. The phase was, however, not so large as ever reported by many authors (JOHNSON, 1967; KANAMORI, 1967; FUKAO, 1977, for example). If such a

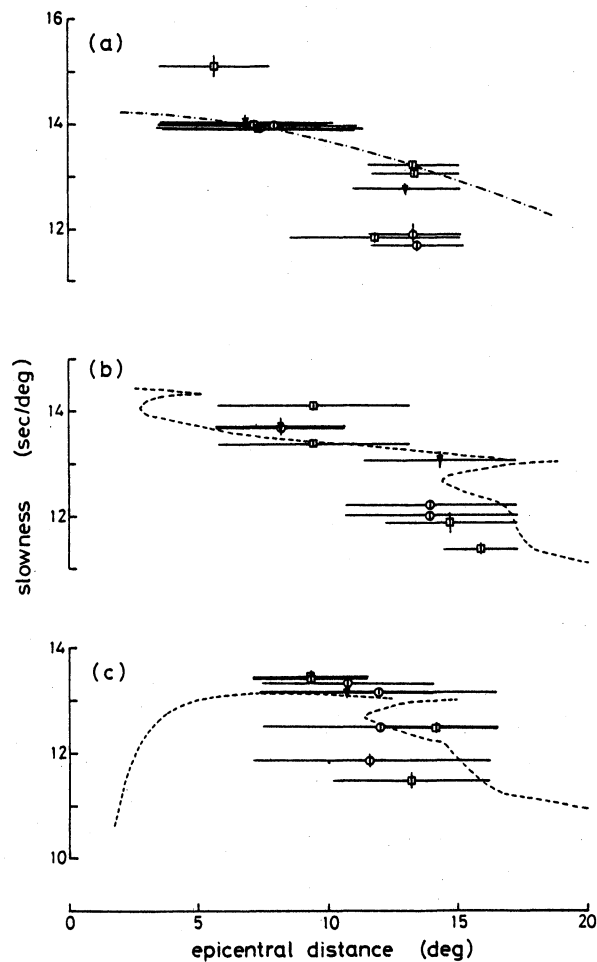


Fig. 21. Summary of P slownesses derived from cross-correlations (circle), cross-spectra (rectangle) and travel times (triangle) compared with theoretical curves: (a) event 2 ( $H = 36\text{km}$ ), (b) event 3 ( $H = 47\text{km}$ ) and (c) event 4 ( $H = 166\text{km}$ ).  $H$ : focal depth. Horizontal line represents the distance range for the measurement and error bar corresponds to the standard deviation. Velocity models refer to K-4-A for events 3 and 4 and to Jeffreys' for event 2.

refraction zone exists, a slowness similar to that of  $P_r$  should be observed for shallow earthquakes in the region but had not been noticed. An interpretation on the phase was given by three-dimensional ray tracing (KAKUTA, 1989):  $P_r$  is refracted from a zone of velocities rapidly increasing between 150 and 180km in the high- $V$  lithosphere in the northeast region.

## 7. Conclusion

Using cross-correlations and cross-spectra, we obtained slownesses agreeing well with those derived from travel times of the first arrival. The measurements were surely reasonable, because slownesses for shallow earthquakes were consistent with  $P_n$  velocities

estimated from explosion seismic observations. Correlation analysis was consequently useful in slowness measurements. It was especially effective for analyzing successive events occurring in a limited region ; reliable estimation was possible by comparing several results.

Slownesses for a phase corresponding to  $P_n$  were 13.3-13.7 s/deg in the northeast region and 13.9-14.0 s/deg in the southwest. For very shallow earthquakes in the northeast, time lag curves of P waves were especially simple and extended linearly from  $4^\circ$  to  $15-18^\circ$  without any clear offset [Figs. 2, 16 and 17]. Such curves are inconsistent with any velocity model including a low velocity layer at a shallow depth.

In contrast, the curve for event 2 in the southwest changed its slope from  $P_n$  to a branch of low slowness at a distance near  $11^\circ$ . The low-slowness phase of 11.7-11.9 s/deg was ascribed to a reflection at the upper boundary of the high- $V$  lithosphere in northeast Japan. On the other hand, large arrival  $P_x$  of 11.5-12.0 s/deg for the earthquakes in the northeast region was interpreted as a phase reflected from a zone of rapidly increasing velocity near 400km depth. In spite of that they were nearly equal in slowness, the time lag curve changed its slope at a distance noticeably shorter for event 2 than for the shallow events in the northeast region.

S phases corresponding to  $P_n$  and  $P_x$  were confirmed on the record sections for a shallow event and an intermediate depth event in the northeast region :  $S_n$  of 23.7-24.5 s/deg and  $S_x$  of 21.1 s/deg. The ratios  $V_p/V_s$  ranged from 1.7 to 1.8.

Although phase  $P_r$  of 12.5 s/deg was detected for the intermediate depth event, clear time gaps ascribable to a low velocity layer was not noticed even on the record sections of S waves. No rapid decrease or increase in amplitude was also observed in the decaying curves. They will probably be explained by the dipping low- $V$  zone convexly curving immediately under the lithosphere.

I would like to thank Prof. Izumi Yokoyama of Hokkaido University (now at Institute of Geophysics, UNAM, Mexico) for his valuable advice and encouragement throughout this work. Prof. Hiroshi Okada, Dr. Ichiro Nakanishi and Dr. Tsutomu Sasatani of Hokkaido University critically reviewed and provided helpful comments. I am also indebted to Dr. Yasuo Sato for suggesting a number of improvements. Thanks are due to several members of the Japan Meteorological Agency, who permitted to copy seismograms.

## REFERENCES

- ARCHAMBEAU, C. B., E. A. FLINN and D. G. LAMBERT, Fine structure of the upper mantle, *J. Geophys. Res.*, **74**, 5825-5865, 1969.
- DRUMMOND, B. J., K. J. MUIRHEAD and A. L. HALES, Evidence for a seismic discontinuity near 200km depths under a continental margin, *Geophys. J. R. astr. Soc.*, **70**, 67-77, 1982.
- FROHLICH, C., M. BARAZANGI and B. L. ISACKS, Upper mantle structure beneath the Fiji plateau : seismic observations of second P arrivals from the olivine-spinel phase transition zone, *Geophys. J. R. astr. Soc.*, **50**, 185-213, 1977.

- FUKAO, Y., Upper mantle P structure on the oceanic side of the Japan-Kurile arc, *Geophys. J. R. astr. Soc.*, **50**, 621-642, 1977.
- GUTENBERG, B., The layer of relatively low wave velocity at a depth of about 80 kilometers, *Bull. Seism. Soc. Amer.*, **38**, 121-148, 1948.
- HASHIZUME, M., O. KAWAMOTO, S. ASANO, I. MURAMATU, T. ASADA, I. TAMAKI and S. MURAUCHI, Crustal structure in the western part of Japan derived from the observation of the first and second Kurayoshi and the Hanabusa explosions. Part 2. Crustal structure in the western part of Japan, *Bull. Earthq. Res. Inst., Tokyo Univ.*, **44**, 109-120, 1966.
- HELMBERGER, D. and R. A. WIGGINS, Upper mantle of midwestern United States, *J. Geophys. Res.*, **76**, 3229-3245, 1971.
- HINO, M., Spectral analyses, *Asakura Syoten*, Tokyo, 1977 (in Japanese).
- IKAMI, A., K. ITO, Y. SASAKI and S. ASANO, Crustal structure in the profile across Shikoku, Japan as derived from the Off Sakaide explosions in March, 1975, *Zisin (J. Seismol. Soc. Japan), Ser. II*, **35**, 367-375, 1982 (in Japanese with English abstract).
- ITO, K., T. YOSHII, S. ASANO, Y. SASAKI and A. IKAMI, Crustal structure of Shikoku, southwestern Japan as derived from seismic observations of the Iejima and Torigatayama explosions, *Zisin (J. Seismol. Soc. Japan), Ser. II*, **35**, 377-391, 1982 (in Japanese with English abstract).
- JOHNSON, L. R., Array measurement of P velocities in the upper mantle, *J. Geophys. Res.*, **72**, 6309-6325, 1967.
- KAKUTA, T., Structure of the upper mantle in the island arc — systematic errors in focal parameters and inspections on the suitability of models, *Rep. Fac. Sci., Kagoshima Univ., (Earth Sci., Biol.)*, **5-6**, 19-60, 1973.
- KAKUTA, T., Q-value in the upper mantle estimated from the decay curve of amplitudes, *Rep. Fac. Sci., Kagoshima Univ., (Earth Sci., Biol.)*, **11**, 81-91, 1978 (in Japanese with English abstract).
- KAKUTA, T., A method of ray tracing in a complicated structure, *J. Phys. Earth*, **33**, 97-119, 1985.
- KAKUTA, T., Revised velocity structure in the upper mantle beneath the Japan region, *Rep. Fac. Sci., Kagoshima Univ., (Earth Sci., Biol.)*, **22**, 119-125, 1989.
- KANAMORI, K., Upper mantle structure from apparent velocities of P waves recorded at Wakayama Micro-earthquake observatory, *Bull. Earthq. Res. Inst., Tokyo Univ.*, **45**, 657-678, 1967.
- KISHIMOTO, Y. and A. KAMITSUKI, On the amplitude of seismic waves observed at the epicentral distance from 6° to 26°, *Zisin (J. Seismol. Soc. Japan), Ser. II*, **9**, 200-217, 1957 (in Japanese with English abstract).
- NAGAMUNE, T., Source regions of great earthquakes, *Geophys. Mag.*, **35**, 333-399, 1971.
- NUTTLI, O., The effect of the Earth's surface on the S wave particle motion, *Bull. Seism. Soc. Amer.*, **51**, 237-246, 1961.
- SASAKI, Y., S. ASANO, I. MURAMATU, M. HASHIZUME and T. ASADA, Crustal structure in the western part of Japan derived from the observation of the first and second Hanabusa explosions, *Bull. Earthq. Res. Inst., Tokyo Univ.*, **48**, 1121-1127, 1970.
- SCHWARTZ, S. Y. and L. J. RUFF, The 1968 Tokachi-oki and the 1969 Kurile Islands earthquakes : variability in the rupture process, *J. Geophys. Res.*, **90**, 8613-8626, 1985.
- UTSU, T., Ratio of  $V_P/V_S$  in the upper mantle beneath the island arcs of Japan, *Zisin (J. Seismol. Soc. Japan), Ser. II*, **22**, 41-53, 1969 (in Japanese with English abstract).